V European Conference on Computational Fluid Dynamics
ECCOMAS CFD 2010
J. C. F. Pereira and A. Sequeira (Eds)
Lisbon, Portugal,14-17 June 2010

A STABILIZED FINITE ELEMENT METHOD FOR COMPRESSIBLE TURBULENT FLOWS

C. Wervaecke*, H. Beaugendre† and B. Nkonga††

*Centre INRIA Bordeaux Sud-Ouest,
Université Bordeaux 1, Campus universitaire de Talence
e-mail: christelle.wervaecke@inria.fr

†IMB - INRIA MC2 - IPB
Université Bordeaux 1, Campus universitaire de Talence
e-mail: heloise.beaugendre@math.u-bordeaux1.fr

††Laboratoire Jean-Alexandre Dieudonné - INRIA PUMAS
Université de Nice - Sophia Antipolis
e-mail: Boniface.NKONGA@unice.fr

Key words: Stabilized finite element, Turbulent flows, Spalart-Allmaras model

Abstract. *In this work, we use a stabilized finite element method to solve Spalart-Allmaras turbulent model for compressible flows. This method is the Streamline-Upwind Petrov-Galerkin one, which enables to put numerical viscosity only along the streamlines. The aim is to build a high order scheme in order not to pollute turbulent eddy viscosity with the diffusivity of the numerical scheme.*

1 Introduction

One of the most important challenge in Computational Fluid Dynamics (CFD) is the simulation of turbulent flows. When high Reynolds turbulent flows are combined with complex and large size geometry, computers are no longer enough powerful to deal with Direct Numerical Simulation (DNS), that is to say with the resolution of all the scales of turbulence motion [1]. Thus, at a fixed scale such as computations can be performed, one have to model the unresolved scales of the turbulence. Although there is an important variety of such models, all of them include intrinsically the turbulent viscosity as a parameter or a variable. Numerical schemes always induce an artificial dissipation that it is crucial to control, such as to be always lower to the viscosity obtained by subscale modeling of the turbulence. High order numerical approximations provide a framework where the constraint on the numerical dissipation can be achieved. Finite elements are suitable for the design of high order scheme with compact stencil that is efficient for parallel computing strategies by domain decomposition and messages passing.

The main weakness of the classical finite element method (Galerkin) is its lack of stability for advection dominated flows. We consider in this work a compressible Navier-Stokes equations combined with the one equation Spalart Allmaras turbulence model. Therefore, the numerical stability is achieved thanks to the Streamline Upwind Petrov-Galerkin (SUPG) formulation [2]. Within the framework of SUPG method, artificial viscosity is anisotropic and the principal component is aligned with streamlines. The aim is to put sufficient viscosity to get rid of instability and unphysical oscillations without damaging the accuracy of the method. The amount of artificial viscosity is controlled by a stabilization tensor τ. Since optimal way to choose τ is still unknown, several ways of computing τ are tested in this paper. Besides SUPG method is also used in combination with a shock-parameter term which supplied additional stability near shock fronts [3].

The remaining of this paper is organized as follows : in Section 2 a description of the Spalart-Allmaras model coupled with the Navier-Stokes equations is given. Section 3 deals with the SUPG formulation for compressible flow. And Section 4 is devoted to the following numerical experiments : first the solution of the flow passing a flat plate at Reynolds number $6.4\ 10^6$ and Mach number 0.24 is compared to the theoretical law of the wall, then the SUPG and the finite volume discretization of the same code are compared on a backward-facing step at Reynolds number 37 000, and finally the solution of a subsonic flow over a S809 airfoil is compared to another published numerical solution.

2 SpalartAllmaras turbulence model for compressible flows

2.1 Navier-Stokes equations

Let $\Omega \subset \mathcal{R}^{n_{sd}}$ be the spatial domain with boundary Γ. The Navier-Stokes equations of compressible flows in the so-called conservative form on Ω can be written as

$$\frac{\partial \mathbf{U}}{\partial t} + \frac{\partial \mathbf{F}_i}{\partial x_i} - \frac{\partial \mathbf{G}_i}{\partial x_i} = 0 \tag{1}$$

where the symbols ρ, $\mathbf{u}$, p and e will represent the density, velocity, pressure, and total energy, respectively, $\mathbf{U} = (\rho, \rho u_1, \rho u_2, \rho u_3, \rho e)$ is the vector of conservative variables, and $\mathbf{F}_i$ and $\mathbf{G}_i$ are, respectively, the Euler and viscous flux vectors.

$$\mathbf{F}_i = \begin{pmatrix} \rho u_i \\ \rho u_i u_1 + \delta_{i1} p \\ \rho u_i u_2 + \delta_{i2} p \\ \rho u_i u_3 + \delta_{i3} p \\ (\rho e + p) u_i \end{pmatrix} \qquad \mathbf{G}_i = \begin{pmatrix} 0 \\ T_{i1} \\ T_{i2} \\ T_{i3} \\ -q_i + T_{ik} u_k \end{pmatrix}$$

Here δ_{ij} are the components of the identity tensor $\mathbf{I}$, q_i are the components of the heat flux vector :

$$\mathbf{q} = -\frac{C_p \mu}{Pr} \nabla T \tag{2}$$

and T_{ij} are the components of the Newtonian viscous stress tensor :

$$\mathbf{T} = \lambda(\nabla.\mathbf{u})\mathbf{Id} + \mu\big(\nabla\mathbf{u} + \nabla\mathbf{u}^t \big) \tag{3}$$

where λ and μ are the viscosity coefficients. It is assumed that $\lambda = -2\mu/3$. The equation of state used here corresponds to the ideal gas assumption. In the case of turbulent regime

$$\mathbf{q} = -\big(\mu + \mu_t \big) \frac{C_p}{Pr} \nabla T \tag{4}$$

$$\mathbf{T} = (\mu + \mu_t)\Big[\big(\nabla\mathbf{u} + \nabla\mathbf{u}^t \big) - \frac{2}{3}(\nabla.\mathbf{u})\mathbf{Id} \Big] \tag{5}$$

Appropriate sets of boundary and initial conditions are set for Eq. (1)

2.2 Turbulence closure model

The turbulent kinematic viscosity $\nu_t = \mu_t/\rho$ is computed using Spalart-Allmaras (S-A) one-equation model. This model is an emperical equation that models production, transport, diffusion and destruction of the turbulent viscosity. In [1], the method is described for incompressible flows. Although there are different approaches to adapt the model for compressible flows, the following one is chosen :

$$\frac{\partial \rho\tilde{\nu}}{\partial t} + \nabla.(\rho\tilde{\nu}\mathbf{u}) = M(\tilde{\nu})\tilde{\nu} + P(\tilde{\nu})\tilde{\nu} - D(\tilde{\nu})\tilde{\nu} \tag{6}$$

where $M(\tilde{\nu})\tilde{\nu}$ represents the diffusion term, $P(\tilde{\nu})\tilde{\nu}$ the production source term and $D(\tilde{\nu})\tilde{\nu}$ the wall destruction source term. The eddy viscosity is obtained from $\tilde{\nu}$ via

$$\nu_t \;=\; \tilde{\nu} f_{v1}\;, \qquad f_{v1} \;=\; \frac{\chi^3}{\chi^3 + c_{v1}^3}\;, \qquad \chi \;=\; \frac{\tilde{\nu}}{\nu} \tag{7}$$

where ν is the molecular viscosity. The production source term is given by

$$P(\tilde{\nu})\tilde{\nu} \;=\; c_{b1}\tilde{S}\rho\tilde{\nu} \tag{8}$$

$$\tilde{S} \;=\; S \;+\; \frac{\tilde{\nu}}{\kappa^2 d^2} f_{v2}\;, \qquad f_{v2} = 1 - \frac{\chi}{1 + \chi f_{v1}} \tag{9}$$

where S is the magnitude of vorticity $\left(S = \sqrt{\Omega_{ij}\Omega_{ij}}, \quad \Omega_{ij} = (\partial_{x_j} u_i - \partial_{x_i} u_j)\right)$ and d is the distance to the closest wall. The diffusion term can be written as

$$M(\tilde{\nu})\tilde{\nu} \;=\; \frac{1}{\sigma}\Big[\; \nabla.\big(\; \sqrt{\rho}(\nu + \tilde{\nu})\nabla(\sqrt{\rho}\tilde{\nu})\;\big) +\; c_{b2}\big(\; \nabla(\sqrt{\rho}\tilde{\nu}).\nabla(\sqrt{\rho}\tilde{\nu})\;\big)\;\Big] \tag{10}$$

And the wall destruction source term is

$$D(\tilde{\nu})\tilde{\nu} \;=\; c_{w1} f_w \rho \left[\frac{\tilde{\nu}}{d}\right]^2 \tag{11}$$

where the wall destruction function f_w is

$$f_w = g\left(\frac{1 + c_{w3}^6}{g^6 + c_{w3}^6}\right)^{1/6}, \qquad g = r + c_{w2}(\; r^6 - r\;)\;, \qquad r = \frac{\rho\tilde{\nu}}{\tilde{S}\kappa^2 d^2} \tag{12}$$

The closure coefficients of the model are $c_{b1} = 0.1355$, $c_{b2} = 0.622$, $\sigma = 2/3$, $\kappa = 0.41$, $c_{v1} = 7.1$, $c_{w1} = c_{b1}/\kappa^2 + (1 + c_{b2})/\sigma$, $c_{w2} = 0.3$, $c_{w3} = 2$.

The wall bounday condition is $\tilde{\nu} = 0$.

2.3 Coupling of Navier-Stokes and Spalart-Allmaras equations

Navier-Stokes equations and Spalart-Allmaras equation are coupled in such a way that, the eddy viscosity is considered as an additional unknown of the system of equations (1). The vector of conservative variables $\mathbf{U}$ becomes $\tilde{\mathbf{U}} = (\; \rho, \rho u_1, \rho u_2, \rho u_3, \rho e, \rho\tilde{\nu}\;)$. Flux vectors $\mathbf{F}$ and $\mathbf{G}$ completed with an extra coefficient for eddy viscosity advection term and diffusion term, respectively, give the new flux vectors $\tilde{\mathbf{F}}$ and $\tilde{\mathbf{G}}$. Finally, the eddy viscosity production and destruction term hold in the vector $\mathbf{S}$.

$$\frac{\partial \tilde{\mathbf{U}}}{\partial t} + \frac{\partial \tilde{\mathbf{F}}_i}{\partial x_i} - \frac{\partial \tilde{\mathbf{G}}_i}{\partial x_i} = \mathbf{S} \tag{13}$$

3 SUPG formulation

The streamline upwind Petrov-Galerkin (SUPG) formulation is one of the most established stabilized formulations and is widely used in finite element flow computations. SUPG method introduces a certain amount of artificial viscosity in the streamline direction only. The aim is to prevent numerical instabilities without introducing excessive numerical dissipation.

3.1 Set of variables

The SUPG method was first introduced using conservative variables [4]. When dealing with a problem of conservative laws such as the Euler equations, the use of conservative variables seems to be a proper choice. Few years later, T.J.R. Hughes et al. [5] introduced a SUPG formulation using entropy variables. The main advantage is that it leads to a symmmetric system, and good properties such as entropy conservation can be proved. However, this set of variables leads to more complicated calculations and Le Beau [6] showed in his works that entropy and conservative variables yield same numerical results. Primitive variables were also proposed by G. Hauke and T.J.R Tezduyar [7] as an acceptable set of variables for the SUPG formulation. They compared entropy and conservative variables with density primitive variables and pressure primitive variables. The numerical solutions showed no significant differences in the case of compressible flow computations.

Since the other set of variables do not lead to better numerical results and conservative variables are much simplier to compute, the followed SUPG formulation is developed using conservative variables.

3.2 Weak formulation

Consider a discretization of Ω into element subdomains Ω_e, $e = 1, 2, ..., n_{el}$, where n_{el} is the number of elements. Each Ω_e is taken to be an open set. Given some suitable finite dimensional trial solution and test funtion spaces $\mathcal{S}^h$ and $\mathcal{V}^h$, the SUPG formulation of Eq. (13) can be written as follows : find $\mathbf{U}^h \in \mathcal{S}^h$ such that $\forall \mathbf{W}^h \in \mathcal{V}^h$

$$\int_{\Omega} \mathbf{W}^h . \left(\frac{\partial \tilde{U}^h}{\partial t} + \frac{\partial \tilde{\mathbf{F}}_i}{\partial x_i} - \frac{\partial \tilde{\mathbf{G}}_i}{\partial x_i} - \mathbf{S} \right) d\Omega + \sum_{e}^{n_{el}} \int_{\Omega_e} \tau \left(\frac{\partial \mathbf{W}^h}{\partial x_i} \right) . \, A_i \, \mathcal{R}(\tilde{U}^h) \, d\Omega = 0 \tag{14}$$

where $\mathcal{R}(\mathbf{U}^h)$ is the residual of the differential equation (13) :

$$\mathcal{R}(\mathbf{U}^h) = \frac{\partial \mathbf{U}^h}{\partial t} + \frac{\partial \mathbf{F}_i}{\partial x_i} - \frac{\partial \mathbf{G}_i}{\partial x_i} - \mathbf{S} \tag{15}$$

The variational formulation (14) is built as a combination of the standard Galerkin integral form and a perturbation-like integral form depending on the residual. τ is the stabilization matrix, various options to compute this parameter were introduced in the literature. This will be discussed in the next section.

3.3 The stabilization parameter

Stabilization parameter has been a subject of an extensive research over the last three decades. Nevertheless, the definitions of τ mostly rely on heuristic arguments and a general optimal way to choose τ is still unknown. Therefore, in this paper, several ways of computing τ are tested.

For the one-dimensional, advection-diffusion, steady case, the following definition of τ yields a nodally exact solution

$$\tau \;=\; \frac{h_e}{2||a||}\left(cothPe - \frac{1}{Pe}\right), \qquad Pe = \frac{||a||h_e}{2\kappa} \tag{16}$$

Where h_e is a measure of the local length scale, also known as "element length", a is the flow velocity, κ is the diffusivity and Pe the Peclet number. In the framework of turbulent flows, problems are convection-dominated : $Pe \gg 1$ and $\coth(Pe) - 1/Pe \;\approx\; 1$. By analogy with formula (16), the parameter τ_1 is then defined by

$$\tau_1 = \frac{h_e}{||\mathbf{u}|| + c}\ \mathrm{Id} \tag{17}$$

Where the acoustic speed is defined as c. The second stabilization parameter proposed reads :

$$\tau_2 = |\Omega_e|\left(\sum_{k=1}^{n_{en}} \mid A_1 n_x^i + A_2 n_y^i + A_3 n_z^i \mid\right)^{-1} \tag{18}$$

$$A_i = \frac{\partial F_i}{\partial U} \qquad \text{in}\ \ \Omega_e \tag{19}$$

Indeed matrices A_i can be considered as a generalization of the scalar advection coefficient for the system of equation (13) . Thus, these matrices can be employed in order to define the stabilization parameter. That is done following an expression coming from a Residual Distribution schemes, the N-scheme[8].

The third option has been proposed by T.E. Tezduyar and M. Senga[3].

$$\tau_3 = \left(\sum_{k=1}^{n_{en}} c|\mathbf{j}.\nabla\phi_k| + |\mathbf{u}.\nabla\phi_k| \right)^{-1} \mathrm{Id} \tag{20}$$

where $\mathbf{j}$ is a united vector define as $\frac{\nabla\rho}{||\nabla\rho||}$, c is again the acoustic speed and ϕ_k are the tests fuctions.

4 Numerical results

4.1 Flat plate boundary layer

The first problem considered is a compressible high Reynolds number flow over a flat plate; see Fig. 1 for the problem description and a view of the discretization used. Values of the CTTM are adopted, namely $C_f = 0.00262$ at $Re_\theta = 10^4$ and a Mach number of 0.24 (which corresponds to a Reynolds number of 6.410^6 for a one meter long flat plate), see Spalart and Allmaras[1] for more informations on the test case.

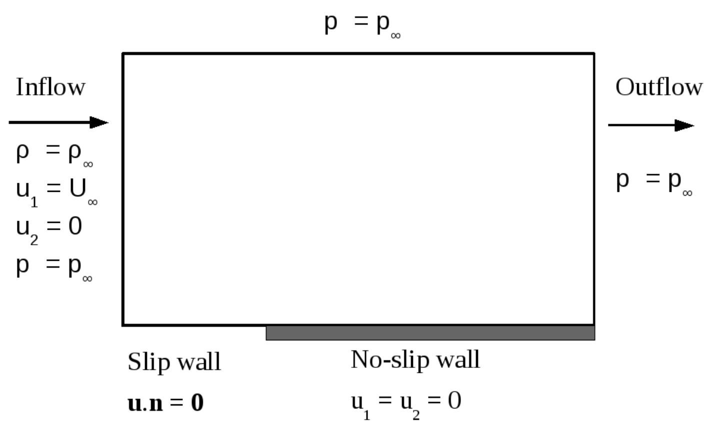

Figure 1: Flow over a flat plate

As it has been the subject of a great deal of researches, the velocity profile of a turbulent boundary layer is well known. The profiles are typically plotted in the so called logarithmic wall coordinates where

$$u^+ = \frac{u}{u_\tau}\ , \qquad y^+ = \frac{u_\tau y}{\nu}\ , \qquad u_\tau = \sqrt{\frac{\tau_w}{\rho}} \tag{21}$$

where $\nu = \mu_{visc}/\rho$ is the kinematic viscosity, τ_w is the shear stress at the wall. In these coordinates the boundary layer can be divided into four distinct regions. Leaving the wall, the first region is known as the viscous sublayer ($y^+ < 5$) and the variation of $u+$ is such that

$$u^+ = y^+ \tag{22}$$

Then, from $5 < y^+ < 50$, the buffer layer provides a smooth transition to the log law $50 < y^+ < 1000$ where

$$u^+ = \frac{1}{\kappa} ln y^+ + C \tag{23}$$

in which $\kappa = 0.41$ and the $C \approx 5.1$. The last region is known as the wake region.

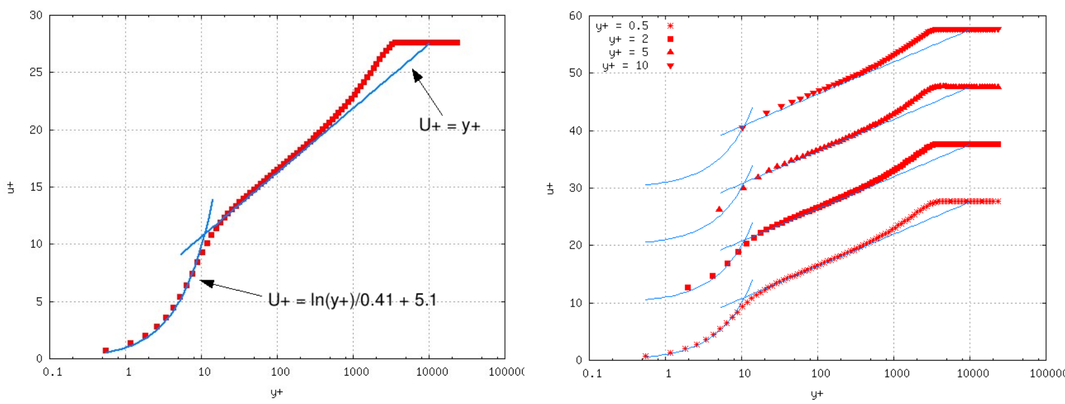

(a) Velocity profile for $y^+ = 0.5$

(b) Velocity profiles for various y^+

Figure 2: Flow over a flat plate. Boundary layer velocity profile

The law of the wall and the log law are plotted with the computed solution (Fig. 2a). Theoretical and numerical results are in good agreement. The mesh employed is viewed as fine. The first layer of nodes next to the wall is at $y^+ = 0.5$. To study the effect of mesh spacing, the closest point to the wall was allowed to vary. Figure 2b illustrates the effect of near wall refinement on the velocity profiles. For the sake of clarity, curves are shifted to the top on figure 2b while in fact, they overlay. There is very little variation in the results. Furthermore, no significant difference in the results has been observed for the three definitions of the stabilization parameter.

4.2 Backward-facing step

The geometry is a 1.33 m long and 0.10 m tall rectangular inlet duct followed by a 0.0127 m rearward-facing step. The test was performed at a freestream velocity of 44.2 $m.s^{-1}$ and atmospheric total pressure and temperature. These conditions correspond to a freestream Mach number of 0.128, a boundary thickness of 1.5H, and a Reynolds number (based on momentum thikness) of 5000 at a location 4 step heights upstream of the step. The Reynolds number based on step height is 37 000. Figure (3a) gives an overview of the flow field obtained, in wich a recirculation is formed downstream of the step, a zoom of the mesh used in this region is represented in figure (3b).

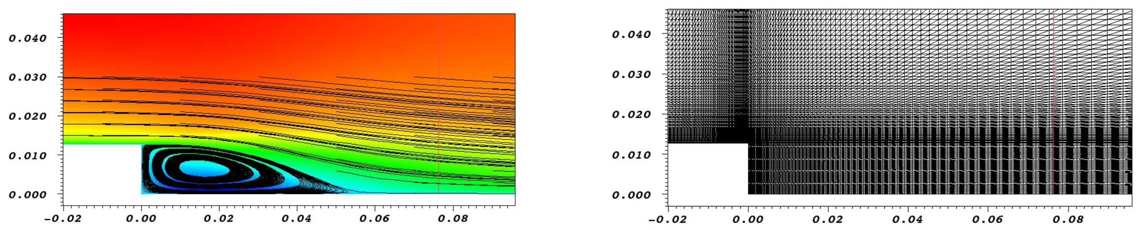

(a) Streamlines of velocity (b) Detail of the domain discretization

Figure 3: Backward-facing step

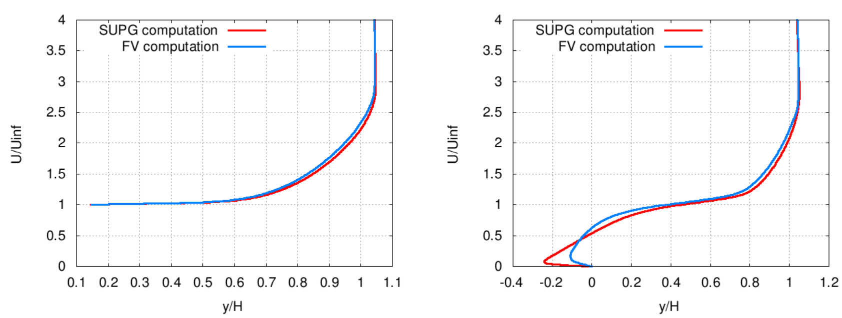

(a) x = -4H (b) x = H

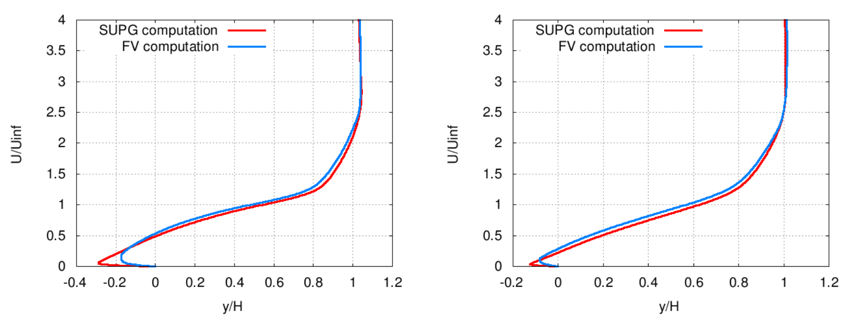

(c) x = 2H (d) x = 4H

Figure 4: Velocity profiles for finite element and finite volume computations

Several computations for this flow have been done. First, the SUPG method is used combined with the stabilization parameters τ_1, τ_2 and τ_3 . Solutions obtained with these different parameters are very similar. Then, a finite volume version of the same code is used to compare the finite volume solution to the SUPG one. Figure 4 represents the velocity profile at several locations in the domain. The fact underlined is that the SUPG method brings less numerical diffusion than a finite volume method. However, the finite volume method can be improved by enlarging the stencil to obtain more accurate results[11]

4.3 Subsonic flow over a S809 airfoil

The problem considered here is a flow over a S809 airfoil. This kind of profil is typically encountered in wind turbine design. The S809 aerodynamic characteristics are well documented in Sommers work[9]. Fully turbulent flow was assumed, Reynolds number is 2×10^6, Mach number is 0.083. The discretization used to calculate this flow employed unstructured elements (see Figure 5).

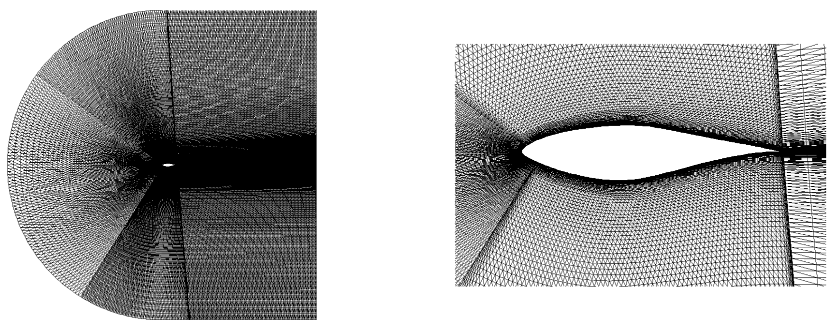

(a) Complete domain discretization

(b) Refinement near the airfoil

Figure 5: Subsonic flow over a S809 airfoil. Discretization : 54 836 nodes, 10 8750 triangles.

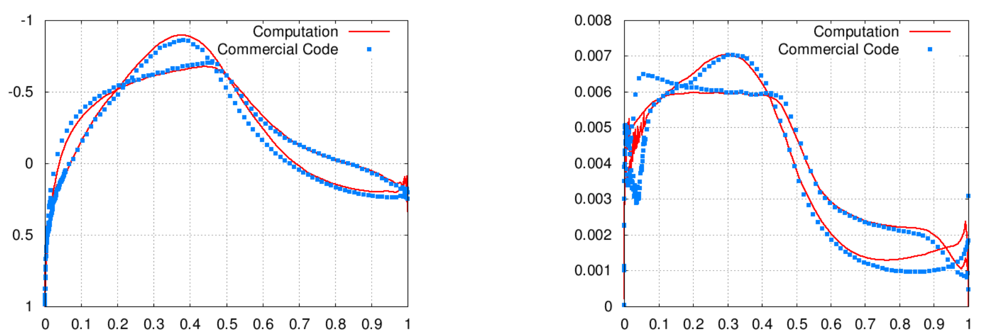

(a) Coefficient of pressure distribution on the airfoil

(b) Skin friction distribution on the airfoil

Figure 6: Subsonic flow over a S809 airfoil.

Figure 6 shows results for the coefficient of pressure C_p and the coefficient of friction C_f, that are in good agreement with results published in 10 and obtained with a commercial code on the same mesh.

5 Conclusion

A stabilized finite element formulation applied to Navier-stokes equation combined with the Spalart-Allmaras model is proposed in this study. Numerical results show that, not only this method is able to reproduce good turbulent profiles in the case of a 2D flat plate, but also that it brings less numerical diffusion than a finite volume method. Even in the case of a almost incompressible flow, the numerical code is robust and gives good results. The choice of the stabilization parameter is yet a problem unsolved, but it seems that the second definition τ_2 performed better with the test cases presented here.

Acknowledgments

Authors acknowledge Airbus France for its support through the DESGIVRE project.

REFERENCES

[1] P. R. Spalart and S. R. Allmaras, A One-Equation Turbulence Model for Aerodynamic Flows, AIAA-92-0439 (1992).

[2] L. P. Franca and G. Hauke and A. Masud, Revisiting stabilized finite element methods for the advectivediffusive equation, *Comput. Methods Appl. Mech. Engrg.*, **Vol. 195**, 1560-1572 (2006).

[3] T. E. Tezduyar and M. Senga, Stabilization and shock-capturing parameters in SUPG formulation of compressible flows, *Comput. Methods Appl. Mech. Engrg.*, **Vol. 195**, 1621-1632 (2006)

[4] T.J.R. Hughes and T.E. Tezduyar, Finite element methods for first-order hyperbolic systems with particular emphasis on the compressible Euler equations, *Comput. Methods Appl. Mech. Engrg.*, **Vol. 45**, 217-284 (1984).

[5] T.J.R. Hughes and T.E. Tezduyar , A new finite element formulation for computational fluid dynamics : I. Symmetric forms of the compressible Euler and Navier-Stokes equations and the second law of thermodynamics, *Comput. Methods Appl. Mech. Engrg.*, **Vol. 54**, 223-234 (1986)

[6] G.J. Le Beau and S.E. Ray and S.K. Aliabadi and T.E. Tezduyar, SUPG finite element computation of compressible flows with the entropy and conservation variables formulations, *Comput. Methods Appl. Mech. Engrg.*,**Vol. 104**, 397-422 (1993).

[7] G. Hauke and T.J.R. Hughes, A comparative study of different sets of variables for solving compressible and incompressible flows, *Comput. Methods Appl. Mech. Engrg.*, **Vol. 153**, 1-44 (1998).

[8] R. Abgrall, Essentially non-oscillatory Residual Distribution schemes for hyperbolic problems, *Journal of Computational Physics*, **Vol. 214**, 773-808 (2006)

[9] D. M. Sommers, Design and experimental results for the S809 airfoil, NREL/SR-440-6918, (1997)

[10] N. Tarchoune, F. Morency and C. Masson, 3D numerical icing simulation on rotating wind turbine, *CFDSC confrence*, Kanata, Ontario, May 2009

[11] C. Debiez, A. Dervieux, K. Mer, B. Nkonga, Computation of unsteady flows with mixed finite volume/finite element upwind methods. *Int. J. Numer. Methods Fluids* 27, No.1-4, 193-206 (1998).